LEAP-ASIA-2018 Centrifuge Test at IFSTTAR

Sandra Escoffier[1*], Zheng Li[1], Philippe Audrain [1]

A b s t r a c t :

In the framework of the LEAP-ASIA-2018 exercise, two dynamic centrifuge tests on a gentle slope of saturated Ottawa-F64 have been performed at the IFSTTAR centrifuge. These tests were conducted in parallel with other tests performed in 9 other centrifuge centers. In addition to the objectives of the LEAP-UCD-2017 (comparison of the experimental results, e.g. effect of the experimental procedure or of test parameters on the results, and providing of a database for numerical modeling), the additional objective was to evaluate, through the tested configuration, the generalized scaling approach describes by Iai et *al.* (2005). In this framework, all the centrifuge teams have performed two type of tests. Considering the same prototype geometry, the first test was performed considering the classical approach used in centrifuge modelling and the second test was performed considering the global scale approach. Following the test matrix and test specifications of LEAP-ASIA-2018, IFSTTAR has performed two model test (test A2, renamed IFSTTAR-1/50-62 and test A3 renamed IFSTTAR-2/25-62). The two tests have been performed on a slope sand with the same relative density (62%) considering a target motion PGA_{eff}=0.3g (1Hz ramp sine at the prototype scale).
In this paper the test set up, the deviation from the specifications such as the experimental set up improvement that have followed the LEAP-UCD-2017 tests are presented in details. The results obtained from the two tests are then provided at the prototype scale for comparison. The obtained input base motion is first presented following by the characterization of the soil through CPT profiles. The responses of the saturated sand slopes for both tests in then detail through the analysis of the pore pressure built up, the acceleration in the soil and the displacement measured through surface markers and embedded sensors. Some preliminary result of the global scaling approach are then discuss.

[1] Department GERS, Laboratory GMG, IFSTTAR, Nantes, France
* Corresponding author: E-mail: sandra.escoffier@ifsttar.fr

1. Introduction

Actual researches in numerical modelling on liquefaction phenomena such as for instance advanced numerical technics based on multiscale approach in large deformation (Callari *et al.*, 2010) highlight the need of experimental database for the calibration and the validation processes. In an effort to improve the quality and reliability of the experimental data, a first series of cross tests was performed in the framework of the LEAP-GWU-2015. The analysis of the results, presented in Kutter *et al.* (2018), highlight that the control of the initial condition and of the ground motion are key points for cross testing.

Following this first step, one of the objectives of the LEAP-UCD-2017 research program was to provide high quality laboratory and centrifuge test data. A total of 10 centrifuge teams were involved in this experimental research work. Following a model specifications document each team has performed a series of dynamic tests on a gentle slope of saturated OTTAWA sand. The objectives of the specifications were to minimize the discrepancies between the experimental procedures followed in each centrifuge team in order to evaluate to quality of liquefaction centrifuge tests and the effects of procedure deviations on the obtained results through cross testing. In addition to this repeatability step, additional tests with different densities and with different second and eventually third base shaking were performed. The objective was to highlight the sensitivity of the response to the soil density and base shaking level. Analysis of the results enables to conclude that the used of standardized centrifuge CPT are more reliable for soil characterization than the density obtained from weight an dimension measurement (Kutter *et al.*, 2018).

For the next step of the LEAP program, LEAP-ASIA-2018, the new results will be included in the previous database and they will be compare to the tendencies observed from the previous stages. In addition, the new objective of this LEAP exercise is to provide data to analyze the effectiveness of the global approach for the tested configuration (i.e. gentle submerged slope of sand subjected to a ramp sine loading). In this framework, each of the ten centrifuge teams have performed centrifuge tests at two different centrifuge levels. The first test was performed considering the classical approach used in centrifuge modelling considering an scaling factor for centrifuge test of η_1 and the second test was performed considering the generalized scaling law approach with a scaling factor for 1g test of μ_2 and a scaling factor for centrifuge test of η_2. For both test the prototype was the same and the scaling factors verified $\eta_1=\eta_2*\mu_2$.

In the following the name of the tests performed have been modify to highlight the test conditions. The test named A2 and A3 in the excel file of the centrifuge test template have been respectively renamed IFSTTAR-1/50-62 and IFSTTAR-2/25-62. The number 62 corresponds the the relative density. The test IFSTTAR-1/50-62 refers to the test performed at 50g considering a virtual test with a scaling factor of 1 and the test IFSTTAR-2/25-62 refers to the test performed at 25g considering a virtual test with a scaling factor of 2.

2. IFSTTAR test specifications and generalized scaling laws

2.1 Target density

Following the LEAP-UCD-2017, it was asked to IFSTTAR to performed centrifuge tests on medium dense OTTAWA sand with a target density of 1654 kg/m^3. Consequently, a new calibration of the pluviation system has been made. The same pluviation set up was used as in the previous LEAP exercise (Figure 1). Due to the French standard the selected sieve has an opening of 1.25 mm. This sieve was attached to an automatic hooper that enables back and forth horizontal movements along the whole length of the container (in the X-direction) and a sand tank placed above the sieve enables to maintained a constant flow during the pluviation process. To obtain the request density two slots with an opening width of 25 mm and an axe to axe distance of 50 mm were selected. The falling height was fixed at 500 mm and the length of the opening was sufficient to cover the whole width of the container (in the Y-direction) avoiding problems of overlapping for the pluviation process. A density of 1645 kg/m3 was obtained (average value obtained during the calibration process from 3 measurements of box density, Figure 1(c)). Considering the average values of the maximum (1756 kg/m^3) and minimum (1475 kg/m^3) densities recently provided by Kutter it corresponds to a relative density of 64,5%. If the initial value considered for the calculation of the relative densities are considered (maximum density 1757 kg/m^3, minimum density 1490 kg/m^3) it corresponds to a relative density of 62% instead of the target of 65%. In the following a density of 62% has been considered to renamed the tests performed by IFSTTAR.

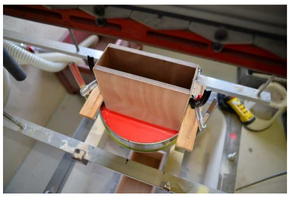

(a) tank of sand

(b) automatic back and forth device

(c) 3 density boxes

Figure 1 Pluviation set up and densities boxes.

2.2 Global scaling laws

Due to the capacity in frequency and acceleration of the IFSTTAR shaker it was asked to performed a first test at 50g centrifuge and a second test at 25g centrifuge, considering respectively a scaling factor for the virtual 1g model of 1 and 2. Due to the global scaling laws, this two configurations should enable to obtained the response of the same prototype. Table 1 summarizes the generalized scaling factors for the tests performed at IFSTTAR.

Table 1 – Global scaling factors for the two tests performed at the IFSTTAR centrifuge

	Scaling factors for 1g test	Scaling factors for centrifuge test	Generalized scaling factors		
			Theoretical expression	IFSTTAR-1/50-63 Scaling factor (μ=1, η= 50)	IFSTTAR-2/25-63 scaling factor (μ=2, η= 25)
Length	μ	η	$\mu\eta$	50	50
Density	1	1	1	1	1
Time	$\mu^{0.75}$	η	$\mu^{0.75}\eta$	50	42
Frequency	$\mu^{-0.75}$	$1/\eta$	$\mu^{-0.75}/\eta$	0.02	0.024
Acceleration	1	$1/\eta$	$1/\eta$	0.02	0.02
Velocity	$\mu^{0.75}$	1	$\mu^{0.75}$	1	1.68
Displacement	$\mu^{1.5}$	η	$\mu^{1.5}\eta$	50	70.7
Stress	μ	1	μ	1	2
Strain	$\mu^{0.5}$	1	$\mu^{0.5}$	1	1.4
Stiffness	$\mu^{0.5}$	1	$\mu^{0.5}$	1	1.4
Permeability	$\mu^{0.75}$	η	$\mu^{0.75}\eta$	50	42
Pore pressure	μ	1	μ	1	2

3. Test configuration and procedure

3.1. Sensor layout and container modifications

In the case of the test performed at IFSTTAR, the inner dimensions of the rigid container are 400 mm(L) x 200 mm (W) x 200 mm (H) (Figure 2(a)). Due to the shaker properties this container is rigidly fixed with 12 screws inside an ESB container which each corner is blocked with a vertical bar. As for the tests performed in the framework of LEAP-UCD-2017, additional sand was put in place between the outer an inner container to reduce the presence of harmonics due the resonance phenomena of the assembly that were observed during the preliminary tests (Figure 2 (b)).

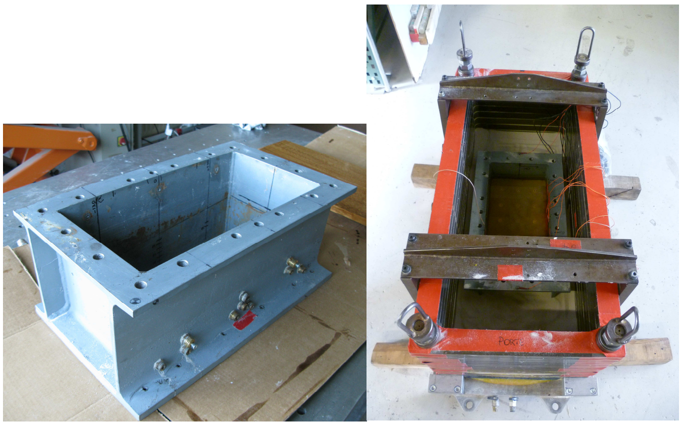

(a) (b)

Figure 2 Rigid steel box especially built for the LEAP project at the IFSTTAR center and placement of the rigid box inside the blocked ESB container.

A cross view and a top view of the sensor layout is presented on Figures 3 and 4 in the case of the test IFSTTAR-1/50-62 (target coordinates). The target coordinates for the test IFSTTAR-2/25-62 are the same.

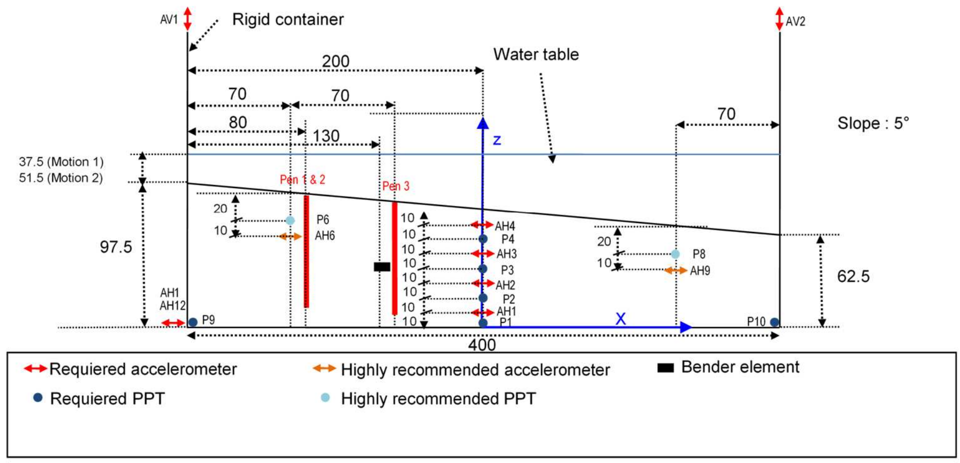

Figure 3 – Cross view of the instrumentation layout of the test IFSTTAR-1/50-62 (target coordinates at the model scale in mm).

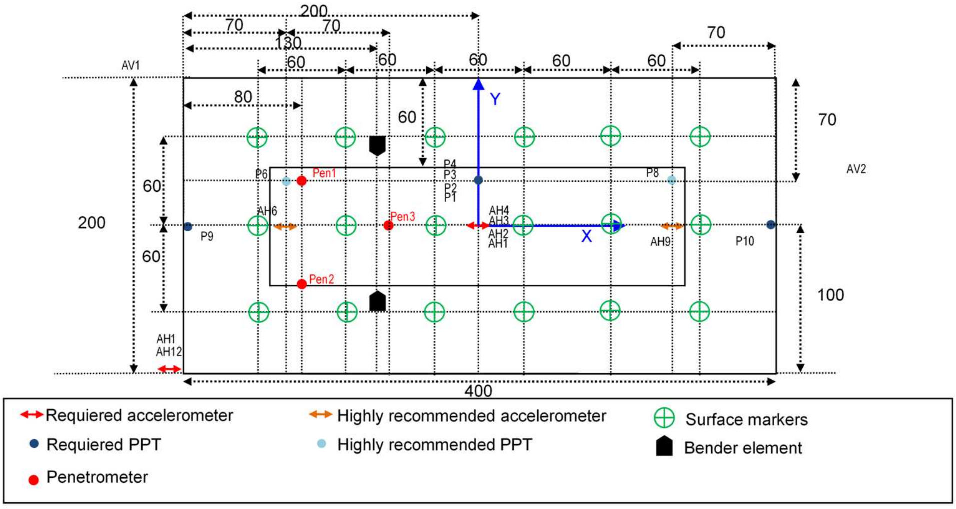

Figure 4 – Top view of the instrumentation layout of the test IFSTTAR-1/50-63(target coordinates at the model scale in mm).

A total of 10 accelerometers, 6 pore pressure sensors, 18 surface markers were used. The same markers as for the LEAP-UCD-2017 were used. The diameter of the surface markers was 2 times smaller than the recommended design (improved design with an external diameter of 13mm). The location of the markers in the X and Y directions were performed with a steel rule with a precision of 1mm and the Z location were performed with a laser sensors. The precision of the Z position is smaller than 0.5 mm as request in the specifications. The surface markers has been put in place before the saturation process and their location has been measured at 1 g before the first spin up of the centrifuge and after each base shaking (Motion#1 and Motion#2) once the centrifuge was spun down.

The shear velocity of the soil was characterized with a pair of bender element that was put in place during the pluviation. The bender elements are of the same type as that described by Brandenberg et *al*. (2006). Measurement has been made before the first event and after each motion. The analysis of the results is currently underway.

In addition, in both containers three CPT tests were made. In each test, the first, second and third CPT characterized respectively the initial state of the soil and the state of the soil after the first and the second base shaking. The CPT used was the one developed at UCDavis (Carey et *al.*, 2018) which has an external diameter of 6 mm. Previously to the centrifuge tests, the CPT was calibrated. The calibration curve highlights an hysteresis and a new calibration will be done. However all the data presented for the CPT test take into consideration this initial calibration.

In the case of the IFSTTAR 1D shaker, the direction of the solicitation is parallel to the axis of the centrifuge (Chazelas et *al.* 2008). From the specifications, the radius between the surface of the soil in a transvers cross section and the center of rotation of the centrifuge should be constant. Consequently, the surface should have a circular shape in the direction perpendicular to the base shaking. However, the distance between the axis of rotation of the centrifuge and the center of the soil surface is 5.063 m. Considering that the inner dimension of the container's width is 0.2m, the difference in height between the midpoint and the corresponding point at the lateral side, should be 1 mm. As this value is in the range of precision of the leveling of the surface the soil surface was not curved in the Y-direction.

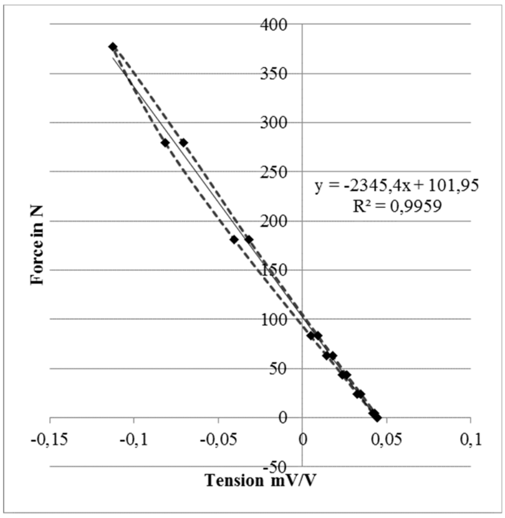

Figure 5 Calibration of the UC Davis CPT.

3.2. Viscous fluid

In order to verify the scaling law and avoid scaling conflict between the velocity of deformation and the diffusion phenomena viscous fluid has been used. This viscous fluid is a mixture of tape water, HMPC (Culminal MHPC50) with and biocide that is added in order to avoid decrease of the viscosity with time (©Kathon biocide).

For the first test the viscous fluid was obtained by mixing 28g/l of HPMC powder with 120ml of Biocide (2% of concentration) and 880 ml of tape water based on a serie of viscosity measurement and the temperature of the centrifuge room. After 5 days, the viscosity was measured between 64 and 60 cst for a temperature of 19°C (measurement at other temperature hasn't been performed due to a problem with the thermostatic bath). At the beginning of the IFSTTAR-1/50-62 test the temperature of the centrifuge room was about 18.5°C. However, due to the small dimensions of the container compared with that of the ESB box usually used it was decided to introduce after the #Motion 1 a temperature sensor in the soil. This sensors was introduce at one of the box corner located at the top of the slope (X=-200mm, Y=100). Due to the length of the sensitive body part of the sensor, the value is representative of a full thickness temperature evaluation of the soil/fluid mixture. After the stabilization, the temperature was measured at 26.7°C. Unfortunately, no viscosity test was performed on the fluid at this temperature during the day of the centrifuge test. After the centrifuge test, viscosity measurement were made but on a fluid taken directly above the soil surface. The viscosity measured was very high between 97 cst at 19°C and 73.07 cst at 26°C. Among the reasons that can explain such large difference between the viscosity before and after the test there is the evaporation. However, the viscosity measurement are sensitives to the presence of impurities. As the fluid was taken above the soils surface, it could have contained impurities. Consequently these values should be considered with caution.

Therefore, for the second test, IFSTTAR-2/25-62, a temperature sensor was introduced at the same location to monitor the temperature before each base shaking. In addition this measurement, in parallel with viscosity measurement, will be done during the next step of the LEAP program to increase the relevance of the viscosity value during the base shaking.

3.3. Saturation process

Compare to the LEAP-UCD-2017 tests performed by IFSTTAR, the saturation system was improved for the LEAP-ASIA-2018 tests. Figure 6 presents the new experimental set up for saturation at 1g. The soil container, the viscous fluid tank and the pump that enables the transfer of the viscous fluid from the tank to the container are all placed in the same vacuum chamber. The lid is a thick plate of Plexiglas that enables to have a top view of all the soil surface during all the saturation process. Once the container, the viscous fluid and the fluid pump in place inside the vacuum chamber, a powerful vacuum pump enables to obtained an absolute pressure of 90 mbars in less than 30 minutes. Once this request absolute pressure is obtained, the vacuum chamber is fill with $C0_2$ up to the atmospheric pressure. Following the saturation process describes by Kutter (2013), the absolute pressure is once again decreases up to 90 mbars and a $C0_2$ flow is once again introduce into the vacuum chamber until the pressure returns to the value of the atmospheric pressure. After a new decrease of the absolute pressure up to 90 mbars, the saturation process starts. As indicated in the LEAP-UCD-2017 specifications, the saturation is made from the surface (at the slope tip) and the fluid pump enables to control the fluid flow all along the process.

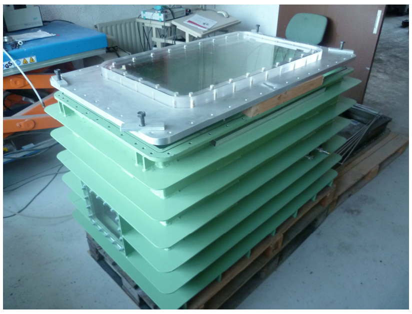

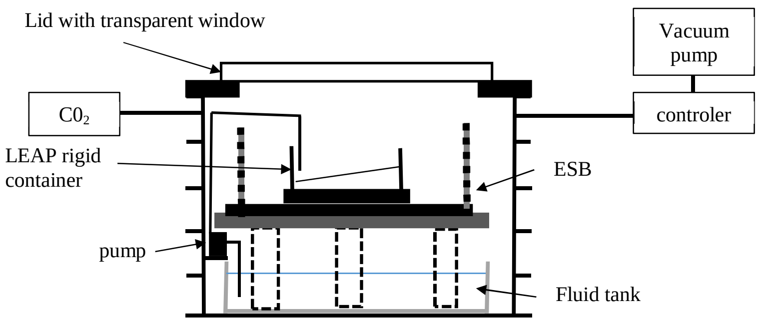

Figure 6 Saturation set up at 1g.

At the end of the saturation process, an attempt to evaluate the degree of saturation was made following the method proposed by Okamura et *al.* (2012). However, the measurement did not enable the determination of the degree of saturation due to the sensor noise and,possibly, to the target and its fixation. This is another point that should be improved for the next LEAP exercise.

As previously indicated the vertical motion of the surface markers were measured using a laser sensors. The use of a laser sensor implies that the source of the laser must be immersed. Due to the minimum distance required between the laser source and the marker the water level should be at least 35 mm above the top of the slope (Figure 3). At the end of the saturation process the fluid level was about 1 cm above the top of the slope, additional viscous fluid was added carefully just before the beginning of the test.

3.4 Wave breaker system

As previously mentioned, due to the use of a laser sensor to record the vertical displacement of the markers between each base shaking a minimum value for height of the water table above the soil surface was necessary. In the previous LEAP-UDC-2017 exercise (Escoffier & Audrain, to be published), an analysis of the pore water pressure variations measured at the bottom of each extremity of the container (P9 and P10, Figure 2) combined with an analysis of the pore pressure variation measured by the sensors located at 1m depth near the extremities (P6 and P8, Figure 2) was made. It was concluded that the amplitudes of the pore pressure measured by these 4 sensors and the fact that a phase opposition was present it could suggest that one part of the pore pressure fluctuations recorded by these sensors was due to the waves. This analysis suggests that a wave reduction system should be built for future tests to avoid non-negligible effect of waves near the extremities of a rigid container.

As a first attempt, a simplified wave breaker was built. Its lower base was in contact with the fluid surface when the container was at rest. The width of the wave breaker was lower than the width of the container. It was assumed that if the wave breaker cover the entire fluid surface it can create unwanted fluid pressure during the base shaking even if it has not been calculated. Consequently the width of the wave breaker was 10 cm.

4. Achieved Ground Motions

4.1 Horizontal Component

Figure 7 gives the time representation of the achieved motions for the 2 motions of each test. The data represents the average value obtained from sensors AH11 and AH12. It should be noticed that in the case of the test IFSTTAR-2/25-62 the time, at which the maximum value of the 1 Hz component is reached, coincides with the time at which the PGA of the raw acceleration is reached. This is not the case for the IFSTTAR-1/50-62 test. In this case the PGA, that is supposed to corresponds to the maximum value of the 1Hz component, has been selected in the time interval [t_0+0.1s, t_0+0.1s] where t_0 is the time at which the maximum value of the 1Hz component is reached. Considering the effective peak ground accelerations, the values measured in the IFSTTAR-2/25-62 are 16 to 25 % higher than that determined in the case of the test IFSTTAR-1/50-62. This difference is essentially due to the level of the noise recorded during the IFSTTAR-2/25-62 that are 64 to 79% higher than that recorded in the IFSTTAR-1/50-62 (Table 2). Figure 8 illustrates the frequency component of the base shaking (average value of the sensors AH11 and AH12). The first 5 most important frequency components are illustrated by red dots and the corresponding frequencies are indicating. At the prototype scale, the frequencies of the harmonics are somewhat different between both tests. However if we consider the values at the model scale for the two first harmonics there are almost the same for both tests: 380 and 449 Hz for the IFSTTAR-1/50-62 against respectively 373 and 458 Hz for the IFSTTAR-2/25-62 tests. One hypothesis can be that these frequencies correspond to resonance frequency of the system assembly that are excited in both tests and due to the generalized scaling law it induces different frequencies at the prototype scale. However, this hypothesis should be confirmed in the future.

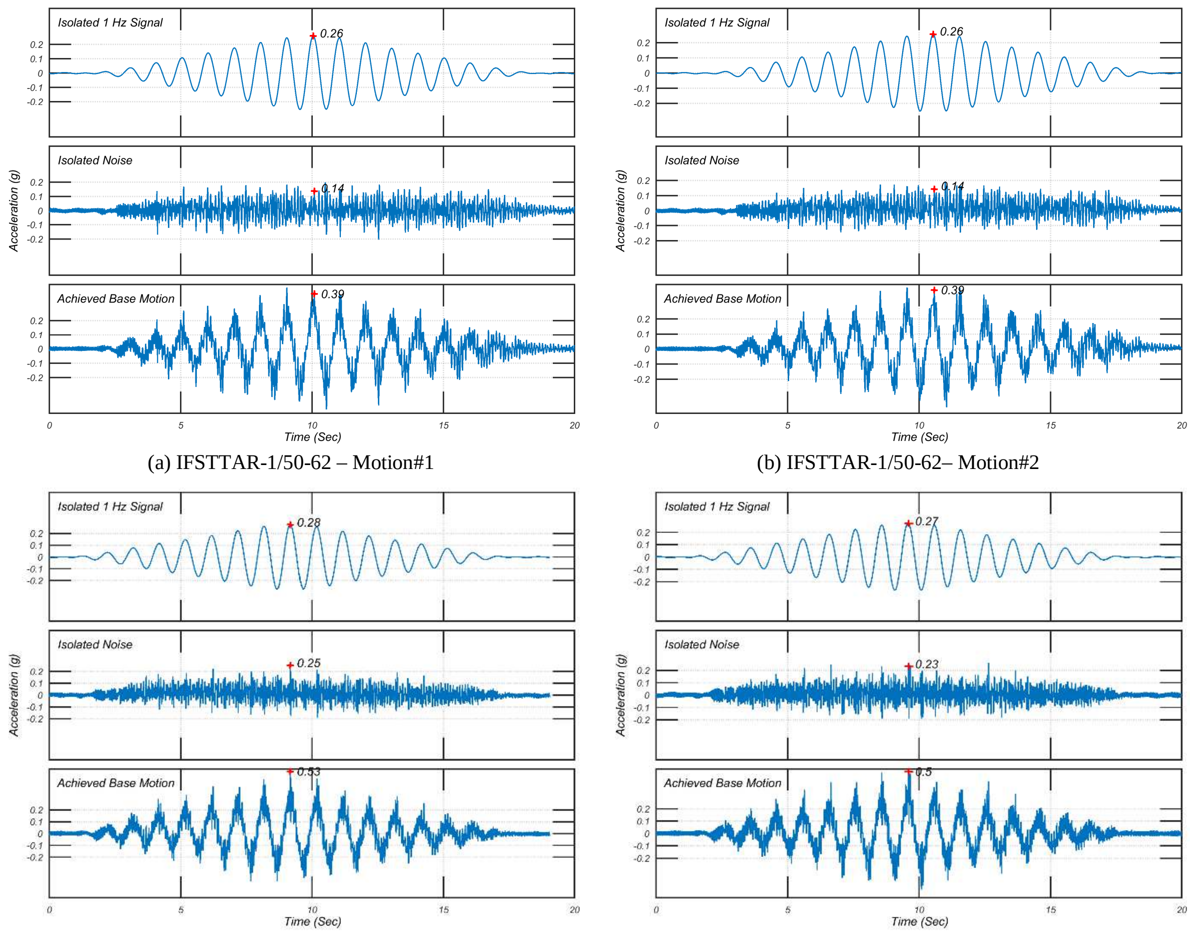

(a) IFSTTAR-1/50-62 – Motion#1

(b) IFSTTAR-1/50-62– Motion#2

(c) IFSTTAR-2/25-62 – Motion#1

(d) IFSTTAR-2/25-62 – Motion#2

Figure 7 Achieved base motions for the two tests performed at IFSTTAR (prototype scale).

If the characterization of the base shaking is based on Arias intensity, the difference between both tests is less important than if the effective PGA is considered. In the case of #Motion 1 and #Motion2, the Arias intensity calculated for the test IFSTTAR-2/25-62 is respectively 13.6 and 8.8 % higher than that calculated for the IFSTTAR-1/50-62 test.

Table 2 – Characteristics of the achieved base motions (prototype scale).

Test	event	PGA eff (g)	1 Hz component (g)	Noise component (g)	3 first main noise frequencies (Hz)*	IA (m/s)
A2 Or IFSTTAR-1/50-63	**#motion 1**	**0.33**	**0.26**	**0.14**	**7.59/8.98/9.63**	**3.95**
	#motion 2	**0.33**	**0.26**	**0.14**	**7.6/8.99/9.67**	**4.19**
A3 Or IFSTTAR-2/25-63	**#motion 1**	**0.41**	**0.28**	**0.25**	**8.95/11/14.99**	**4.49**
	#motion 2	**0.385**	**0.27**	**0.23**	**8.97/10.97/14.98**	**4.56**

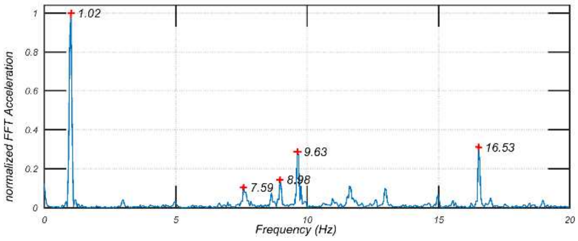

(a) IFSTTAR-1/50-63 – Motion#1

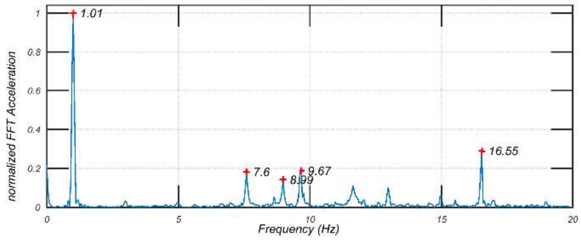

(b) IFSTTAR-1/50-63– Motion#2

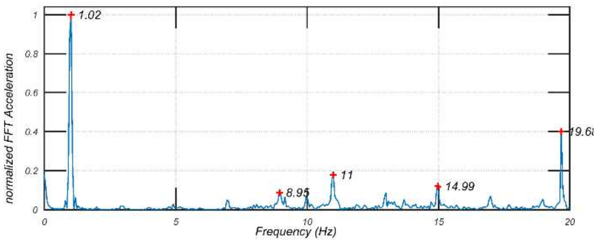

(c) IFSTTAR-2/25-63 – Motion#1

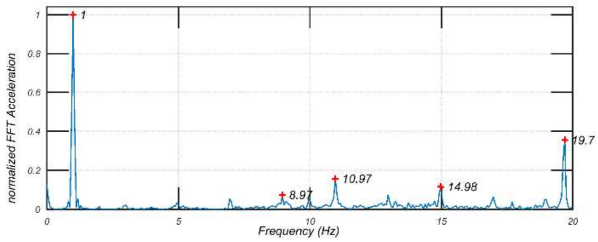

(d) IFSTTAR-2/25-63 – Motion#2

Figure 8 Frequency content of the achieved base motions for the two tests performed at IFSTTAR (prototype scale).

4.2 Vertical Component

The time representation of the vertical components measured at the top of each extremity of the container (AV1 and AV2, Figure 3) is given in Figure 9. Following the analysis of the vertical component made by Kutter *et al.* (2018), a pass band filter [0.3Hz-3Hz] has been applied to the raw data for analysis. A FIR filter was used. Considering all the test the maximum vertical filtered acceleration remains lower than 0.015 g. However, the vertical behavior is not constant. In the test IFSTTAR 1/50-62 for the #Motion 2 there is a phase opposition that indicate a rotation of the container. In the same test for the #Motion 1 the vertical acceleration is not the same at both extremity but there are in phase. For the second test, IFSTTAR 2/25-62, the vertical acceleration are somewhate the same and in phase for the #Motion 1 whereas they are different and present a phase difference for #Motion 2.

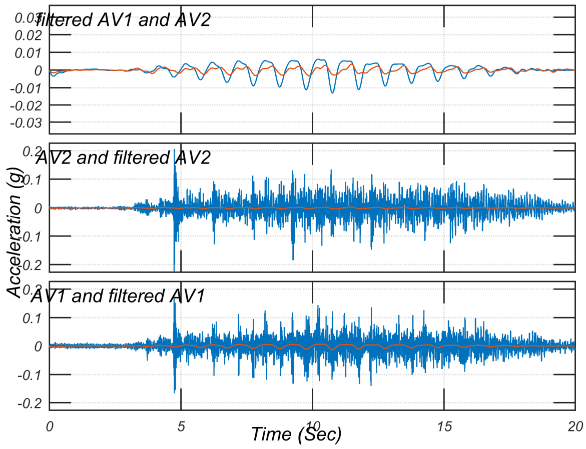

(a) IFSTTAR-1/50-63 – Motion#1

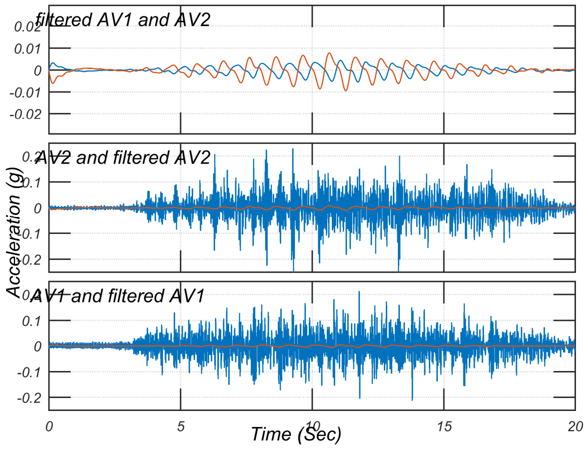

(b) IFSTTAR-1/50-63– Motion#2

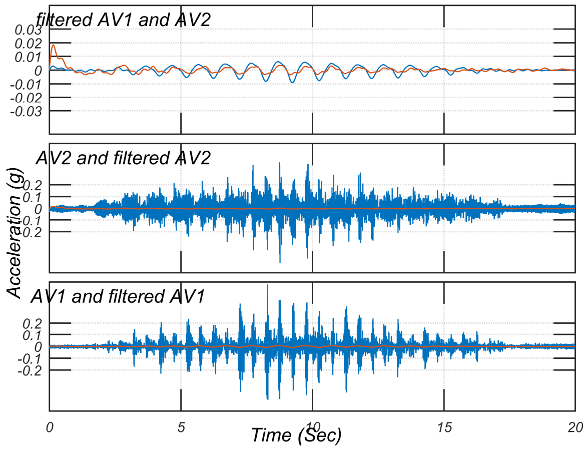

(c) IFSTTAR-2/25-63 – Motion#1

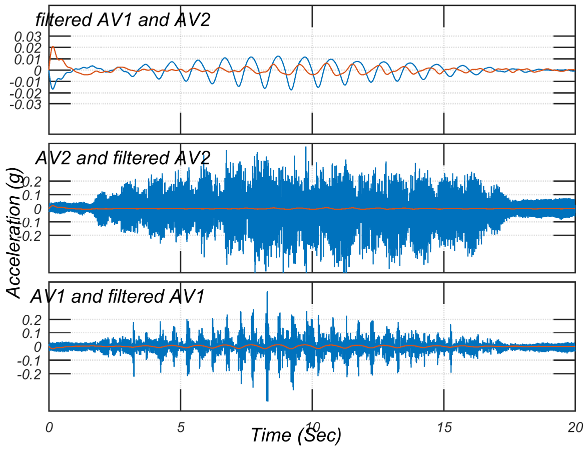

(d) IFSTTAR-2/25-63 – Motion#2

Figure 9 Time representation of the vertical raw and filtered accelerations at both extremities of the rigid container (prototype scale).

5. Results

In this part, all the data are presented at the prototype scale using the generalized scaling laws presented in Table 1.

5.1 CPT test results

The CPT profiles are presented in Figure 10 for each test. In the case of the test IFSTTAR-2/25-62, the depth of investigation was lower than for the other test and the recorded data were noisy.

No noticeable evolution is recorded between the CPT test performed at the initial state and after both motions in the case of the IFSTTAR-2/25-62 test. The $q_c(z)$ profile is almost the same $q_c(z)$ profile that was obtained for the initial state of the soil column in test IFSTTAR-1/50-62. For this last test, successive base shakings induce a modification of the q_c profile: the profile increases with successive shaking indicating a densification of the soil. This result is in accordance with the liquefaction phenomena. Note that the peak that appear in the case of the q_c profile for the initial state of test IFSTTAR-1/50-62 is supposed to be due to the presence of a cable of a pore pressure sensors.

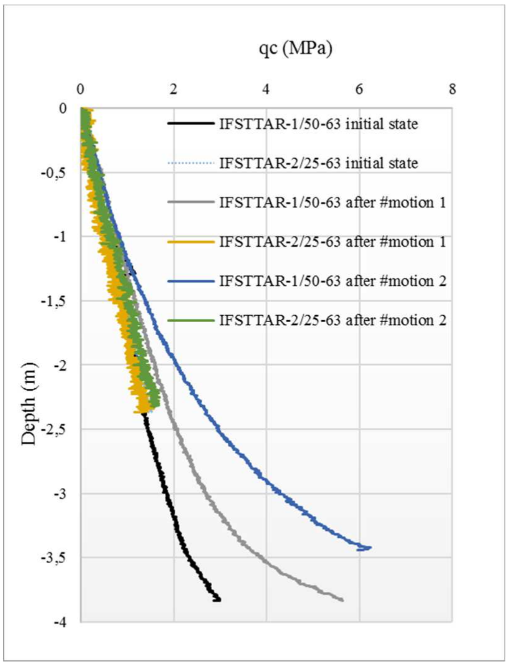

(a)both IFSTTAR tests

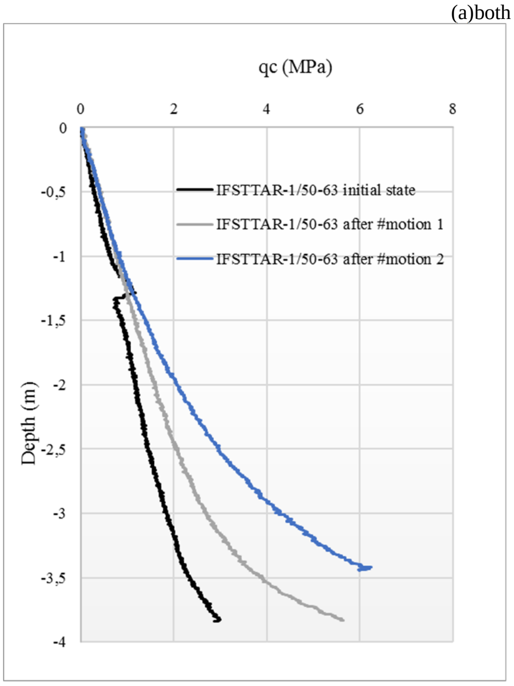

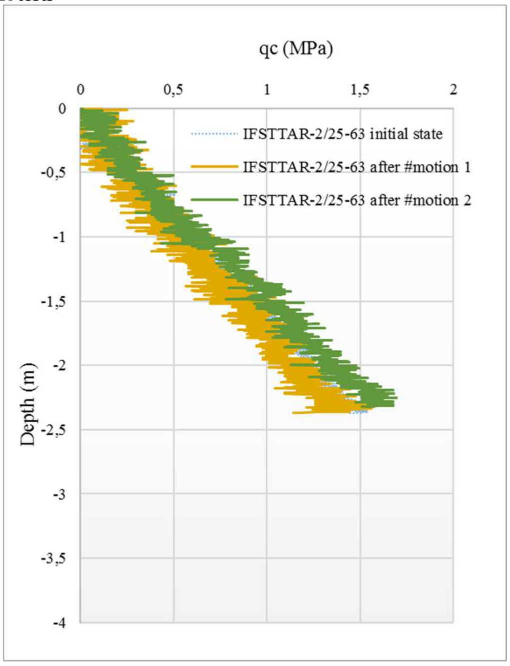

(b) IFSTTAR-1/50-62 test

(c) IFSTTAR-2/25-62 test

Figure 10 – CPT test results for both IFSTTAR test at the prototype scale.

5.2 Pore Pressure Response

Figure 11 shows the pore water pressure response of the central array of pore pressure sensors. Considering the positioning of the sensors during the pluviation process, the initial vertical effective stress for the P1 and P3 sensors in the case of the IFSTTAR-1/50-62 test were respectively 38.9 and 18.2 kPa. In the case of the tests IFSTTAR-2/25-62 the initial vertical effective stress for P1 to P4 were respectively 38.9, 30.3, 23.7 and 9.1 kPa. These limits are indicated in dotted black horizontal lines in Figure 11.

The evolution of the pore pressure observed from P1 and P3 are comparable in both tests. The pore pressure built up is a little noisier in the case of the test IFSTTAR2/25-62. In the case of #Motion 1 in both tests the pore pressure built up reach the initial effective stress at 2m depth. At 4m depth the pore pressure built up is somewhat lower than the initial vertical effective stress, and the value of ru =1 is only reach on a very limited time (this value is only reach for few pore pressure peaks in case of IFSTTAR-2/25-62, and the maximum value of ru reached for IFSTTAR-1/50-62 is 0.96).

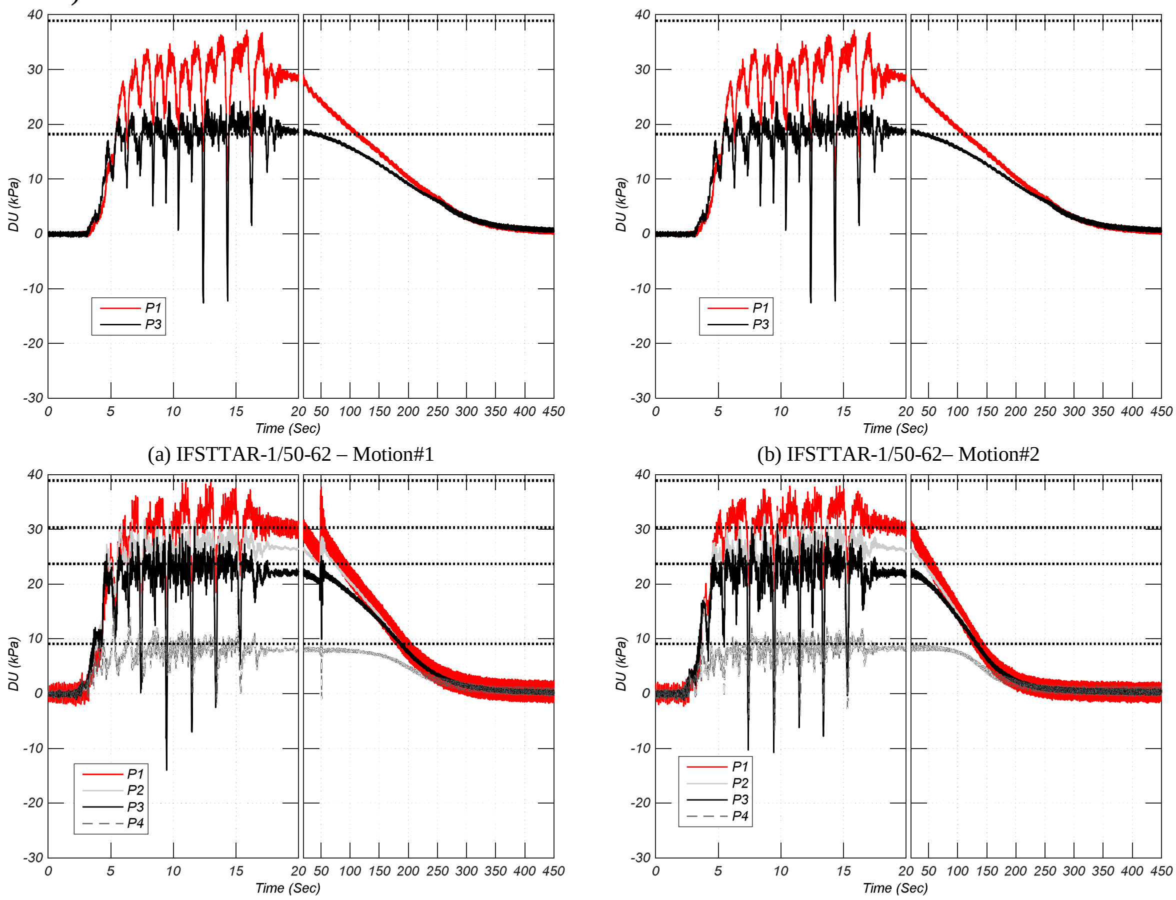

(a) IFSTTAR-1/50-62 – Motion#1

(b) IFSTTAR-1/50-62– Motion#2

(c) IFSTTAR-2/25-62 – Motion#1

(d) IFSTTAR-2/25-62 – Motion#2

Figure 11 Pore pressure built up during and after the base shaking.

In the case of IFSTTAR-2/25-62, the pore pressure built up recorded at 3 and 1 m depth indicate liquefaction (ru=1) for these both levels.

In addition, for both tests some spikes appears during #Motion 1,more especially at 2 and 3 m depth indicating a deliquefaction phenomenon (cyclic mobility – dilatancy phenomena).

Finally, no noticeable evolution is highlighted, from pore pressure measurement between the first and the second motion in both tests.

Concerning the pore pressure decay after the base shaking, it is somewhat difficult to compare both tests in the case of the first motion as, in the case of the IFSTTAR-2/25-62 test an aftershock took place inducing new pore pressure built up. However, in the case of #Motion 2, the pore pressure decay is longer in the case of the tests IFSTTAR-1/50-62. As previously mentioned, uncertainties exist on the viscosity of the fluid in the case of this test. After the test the viscosity has been measured at 73.07 cst but on fluid sample took on the fluid layer above the soil surface. Despite some doubts on the relevance of these measurements, it can be supposed that the viscosity was higher than requested (50cst).

As mentioned for the previous tests performed in the framework of the LEAP-UCD-2017, regarding the amplitude and the phase of the pore pressure measured by pore pressure sensors P10, P9 P8 and P6 (Figure 2), and their initial depth it was supposed that one part of the pore pressure fluctuations recorded by these four sensors was due to the waves created during the base shaking. This previous results suggested the use of a wave breaker system to avoid non-negligible effect of waves near the extremities of a rigid container (the pore pressure measurement located in the center of the container were less influenced by the waves). Consequently, a wave breaker was built for the LEAP-ASIA-2018. Figure 12 illustrates the pore pressure evolution measured by sensors P10, P9, P8 and P6 (Figure 2) during the Motion#1 of the test IFSTTAR-2/25-62 (the same behavior was observed for #Motion2). Sensors P9 and P10, and sensors P6 and P8 are respectively in phase opposition. The maximum pore pressure value recorded by sensors P10, P9, P8 and P6 are respectively 112, 143, 87 and 59 kPa. Considering their initial position and the level of water at rest, the maximal pore pressure (ru=1) are respectively 100, 111, 65 and 50kPa.

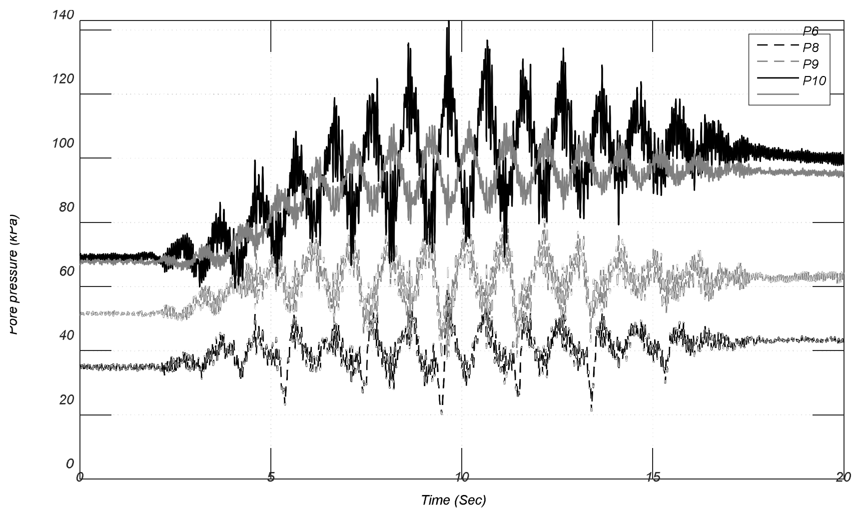

Figure 12 LEAP-2/25-62 #Motion 1 Pore pressure built up during and after the base shaking – wave breaker effect.

In the case of the #Motion 1 of the test IFSTTAR-1/50-62, the wave breaker was not in place. Figure 13 represents the pore pressure measurement P9, P8 and P6 (P10 was out of order) during the #Motion 2. The three pore pressure measurement are in phase. Compare to the theoretical maximal pore pressure 116, 50 and 49 kPa for respectively P9 P8 and P6 the measured ones are somewhat higher (119, 62 and 68 kPa).

The comparison of these two results highlight a difference of behavior between the two tests: if the measured pore pressure remains higher than the theoretical one in both tests, the phase difference between the pore pressure measurements are not the same. Results from the test IFSTTAR-2/25-62 seems to indicate the presence of wave and at contrary there is no clear evidence of waves in test IFSTTAR-1/50-62. For further test, the wave breaker system will need improvements.

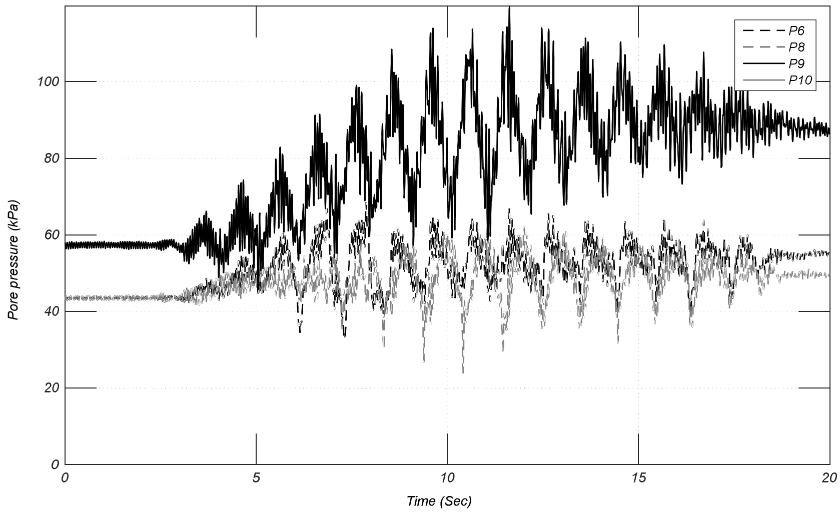

Figure 13 LEAP-2/25-62 #Motion 1 Pore pressure built up during and after the base shaking – wave breaker effect.

5.3 Acceleration response

The time history of the acceleration measured by accelerometers AH1 to AH4 are presented in Figures 14 and 15 for respectively the tests IFSTTAR-1/50-62 and IFSTTAR-2/25-62. The global behavior observed in both tests is comparable.

At the beginning of #Motion 1 the time acceleration at 3.5 m depth in the central array of accelerometers still follow the trace of the base input motion. However after 4 cyclic loadings small spikes start to appears and even if cyclic variation of acceleration are still noticeable they deviate from the base shaking. At 2.5m depth, and above, the initiation of liquefaction can be observed. It is characterized by sharp spikes of acceleration. Considering the beginning of the loading, the liquefaction occur first near the surface and then the phenomenon is spreading in depth. However, there is small phase lag between 0.5 and 2.5 m depth.

There is no noticeable effect of the #Motion1 on the pore pressure observed in #Motion2. The only difference is in the level of deliquefaction spikes that are somewhat lower in the case of #Motion2.

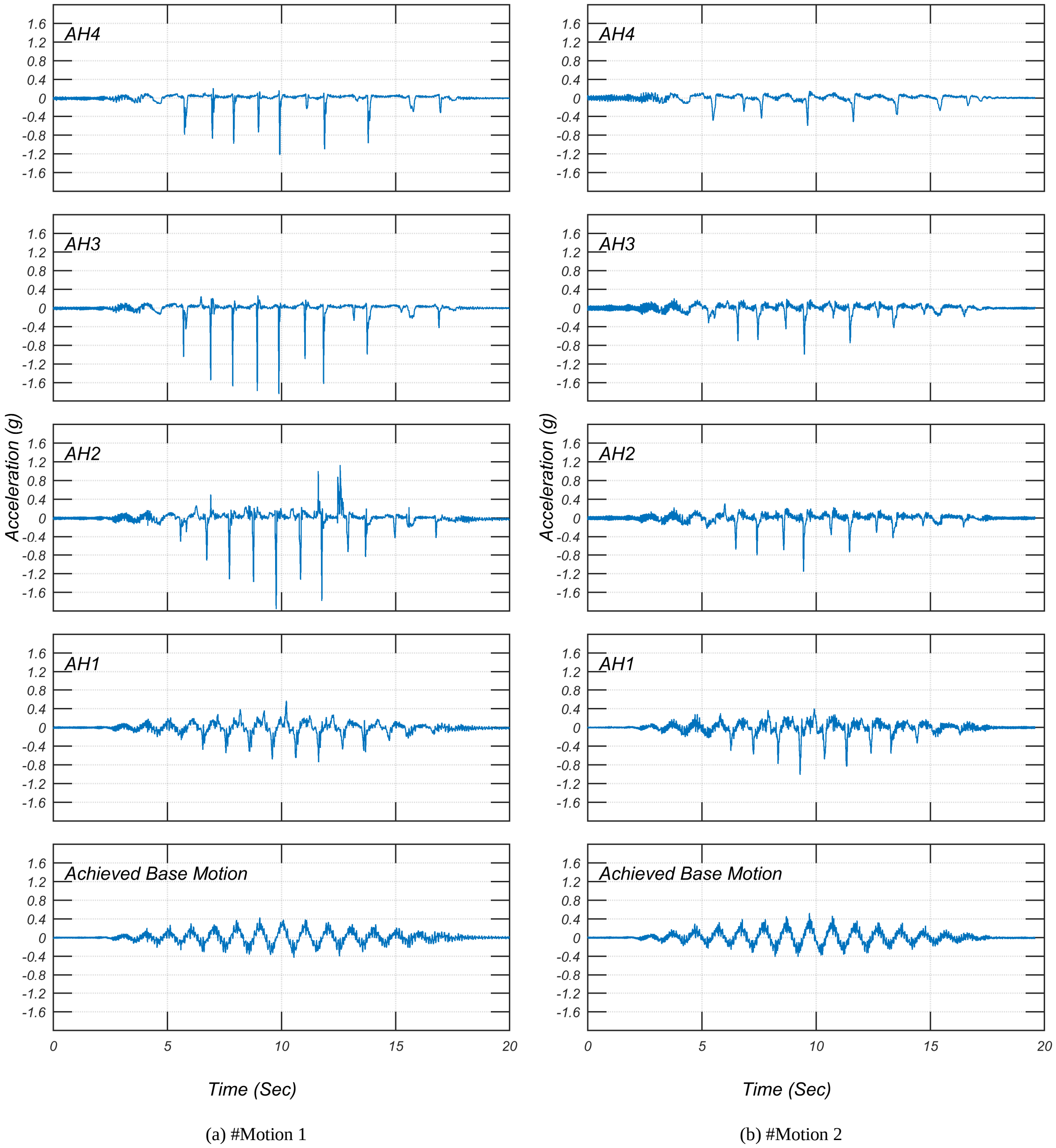

Figure 14 – IFSTTAR-1/50-62 : Time history of the acceleration measured by the central array of accelerometers

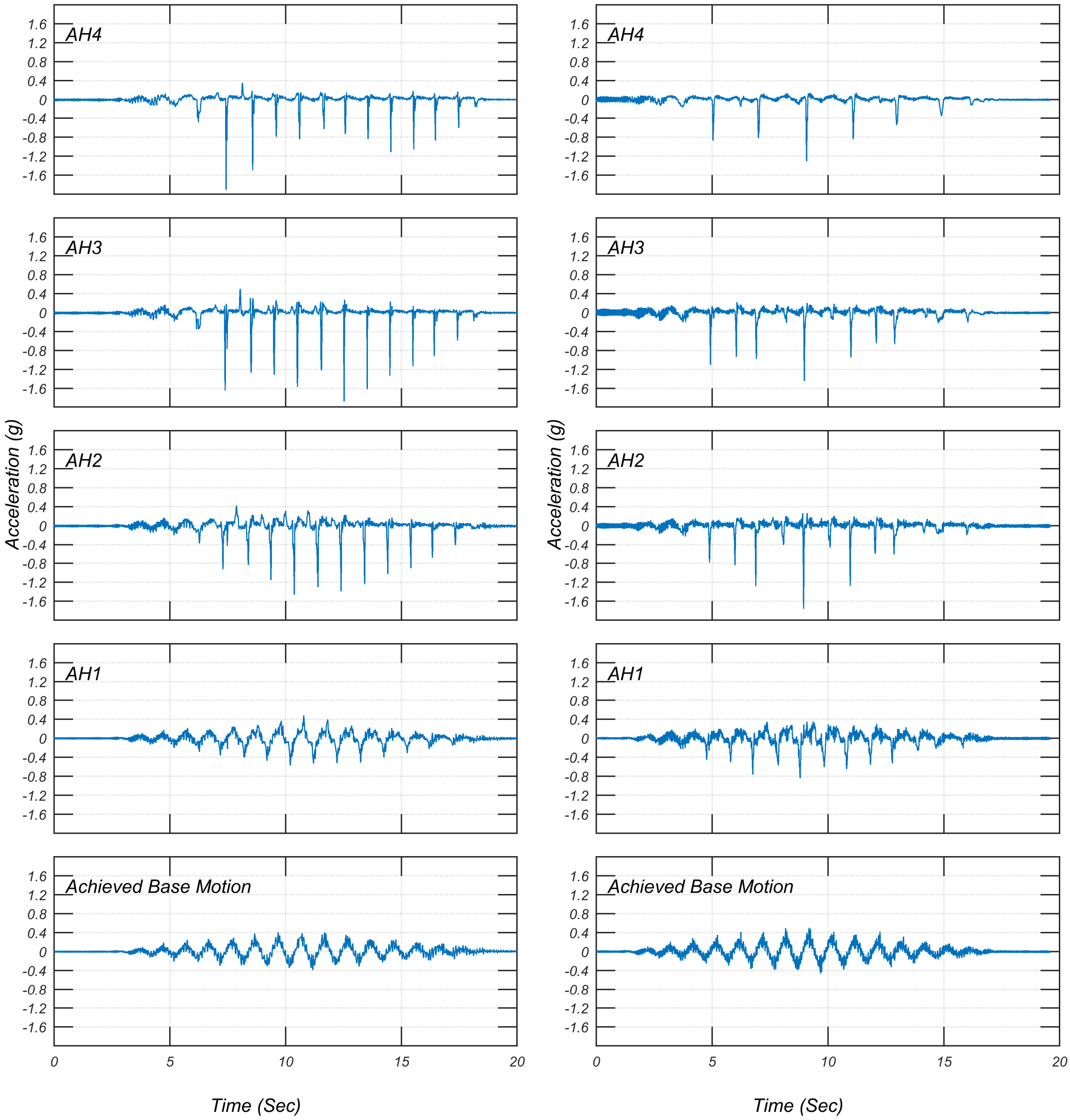

(a) #Motion 1 (a) #Motion 2

Figure 15 – IFSTTAR-2/25-62 : Time history of the acceleration measured by the central array of accelerometers

5.4 Surface Maker Response

A cross view and a top view of the initial position and the vector of the total displacement of the surface markers and embedded sensors are presented on Figure 16. The initial position is the one that corresponds to the first location measurement before the first spin up of the centrifuge for the surface markers and during the pluviation process for the embedded sensors. The final location measurement corresponds to the location measured after the second base shaking once the centrifuge was spin down for the surface markers and during the dismantle of the container for the embedded sensors. In order to enhance the displacement and compared the results of both tests, the length of the displacement vector was magnified by 3.
In the case of the surface displacement induce by #Motion 1, the direction of the displacement are somewhat the same in both tests (Table 3). However, larger displacement are observed in the case of the test performed at 25g centrifuge and for the which one the generalized scaling law are used (29 to 139 % larger, Table 3).

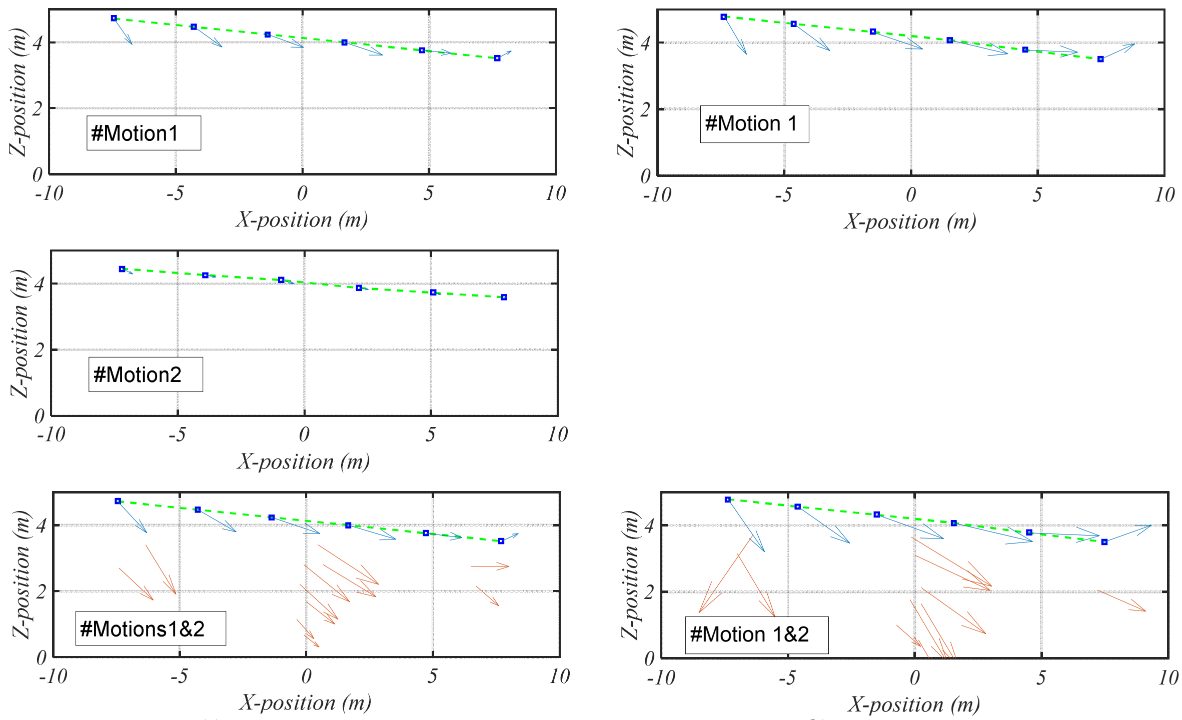

(a) IFSTTAR-1/50-62
(b) IFSTTAR-2/25-62

Figure 16 Surface markers (blue arrows) and embedded sensors displacement (red arrows) induce by #Motion 1, #Motion 2, #Motion 1 & 2, for both centrifuge tests performed at IFSTTAR.

In order to highlight the effect of previous base shaking on the surface displacement the displacement associated with the second base shaking are represented in the case of the test IFSTTAR-1/50-62. The observed displacement are largely lower than that induce by the first event. This decrease can be due to densification of the soil between both motions. This analysis is more complex in the case of the test IFSTTAR-2/25-62 due to scaling conflict between the displacement and the length. Consequently, only the total displacement induce by the combined effect of both motions is represented for both tests. In this case, the total motion of the embedded sensors are also represented. The difference between the displacement amplitude and their orientation between the two tests are comparable to that observed for the first motion (Table 4). In the case of the test based on double scaling approach the displacement are 38 to 68% higher than in the other test with larger difference at the bottom of the slope. The difference in the direction varies between 6 to -67% indicating that at the top of the slope the soil movement is more downward and near the bottom of the slope more upward for the test IFTTAR-2/25-62.

Table 3 – Average displacement amplitude and orientation calculated from the measured displacements of the surface markers – #Motion 1.**

#Motion 1	Amplitude (m)			Orientation(°)		
Marker number	IFSTTAR-1/50-63	IFSTTAR-2/25-63	Relative difference in %*	IFSTTAR-1/50-63	IFSTTAR-2/25-63	Relative difference*
1	0.358	0.483	35	-47.5	-52.4	10
2	0.419	0.542	29	-28.9	-29.6	2
3	0.493	0.682	38	-15.4	-14.5	-6
4	0.517	0.778	50	-14.6	-10.23	-30
5	0.384	0.696	81	-4.1	-1.8	-56
6	0.198	0.473	139	22	18.7	-15

* The relative difference is calculated taking into account the IFSTTAR-1/50-63 test as a reference

** the values correspond to the average value of the displacement amplitude and inclination calculated from the three marker located at the same x-position.

Table 4 – Average displacement amplitude and orientation calculated from the measured displacements of the surface markers #cumulative effect of motions 1 and 2.

#Motion 1 & 2	Amplitude (m)			Orientation(°)		
Marker number	IFSTTAR-1/50-63	IFSTTAR-2/25-63	Relative difference*	IFSTTAR-1/50-63	IFSTTAR-2/25-63	Relative difference*
1	0.498	0.714	43	-39.7	-47.4	19
2	0.547	0.774	41	-24	-28.0	17
3	0.662	0.916	38	-14.4	-15.2	6
4	0.642	1.054	64	-13.0	-10.2	-22
5	0.477	0.932	95	-5.4	-1.8	-67
6	0.237	0.636	168	18.6	15.4	-17

6. Conclusion

This paper summarized the built up and some results of the two centrifuge tests performed at IFSTTAR in the framework of the LEAP-ASIA-2018 series of tests.

Two centrifuge tests were performed by IFSTTAR, the tests were done on a dense and a medium loose Ottawa-F65 sand. The first test was performed at 50g centrifuge and the second test at 25g. Considering the generalized scaling law approach, tests were scaled to represent the same prototype.

The main deviation from the specifications was the viscosity of the fluid for the IFSTTAR-1/50-62 test for which one the viscosity is assumed higher than the request one, despite no precise determination is available. This assumption seems verified if the time dissipation of the pore pressure built up is considered.

Compared to the previous tests performed in the framework of LEAP-UDC-2017 exercise an improved system of saturation was used which enables a better controls of the fluid flow and less leakage due to its configuration.

The 1 Hz horizontal component of the base shaking at the base of the container was similar between the tests. The noise was somewhat higher in the case of the IFSTTAR 2/25g-62 test inducing a PGA_{eff} 15 to 25 % higher than for the IFSTTAR-1/50-62. This difference decreases to 13.6 up to 8.8% if the Arias intensity is considered.

The vertical motion at the top of the container wasn't constant between the test and between the motion of each test. Difference between the tests can be due do the difference of frequency for the base shaking that can induce different response of the assembly. However the difference of response between the motions of the same test is not actually explained.

Considering the results obtained, the characterization of the soil column through CPT measurement highlights a difference between the two tests. However, the noisy response obtained for the second test can be relevant of the problem with the experimental set up in this case. For the next LEAP exercise, a new calibration of the CPT will be made and more caution will be taken for the CPT tests.

The global scaling approach seems to give good results if the acceleration and the pore pressure built up are considered. However due to a problem with the fluid viscosity these tests are not relevant for the analysis of the global scaling approach when it concerns the pore pressure dissipation after the base shaking.

At the contrary when the displacement are considered large discrepancy appears especially in terms of amplitude and, to a lesser extent, in terms of orientation.

7. Acknowledgements

This experiment has been made in the framework of the LEAP-ASIA-2018 series of experiments. The authors would like to thank all the participating centrifuge teams that share their knowledge.

8. References

Brandenberg, SJ, Choi S, Kutter BL., Wilson DW, Santamarina, JC. A Bender Element System for Measuring Shear Wave Velocities in Centrifuge Models. Proceedings, 6th International Conference on Physical Modeling in Geotechnics, 2006, p 165-170. https://nees.org/data/get/NEES-2006-0149/Documentation/References/Brandenberg_2006.pdf

Callari C., Armero F. Abati, A. Strong discontinuities in partially saturated poroplastic solids. Comput. Methods Appl. Mech. Engrg., 2010, pp. 1513-1535.

Carey T, Gavras A, Kutter B, Haigs SK, Madabushi SPG, Okamura M, Kim DS, Ueda K, Hung WY, Zhou YG, Liu K, Zeghal M, Abdoun T, Escoffier S, Manzari M. A new shared miniature cone penetrometer for centrifuge testing. ICPMG 2018 MCNamara A Divall S Goodey R Taylor N Stallebrass S & Panchal J Eds. London , 2018, Vol. 1, p 293-298.

Chazelas, J.-L., Escoffier, S., Garnier, J., Thorel, L., Rault, G. Original technologies for proven performances for the new LCPC earthquake simulator, Bulletin of Earthquake Engineering, Vol. 6 n°4, 2008, pp. 723-728.

Escoffier S, Audrain P. LEAP-UCD_2017 Centrifuge Test at IFSTTAR. LEAP-UCD-2017: *Reproducibility and sensitivity of centrifuge tests and comparisons to simulations of lateral spreading*, to be published, PP. XXX.

Iai S, Tobita T, Nakahara T. Generalised scaling relations for dynamic centrifuge tests. Géotechnique 55(5), 2005, p.355-362.

Kutter BL, Carey TJ, Hashimoto T, Zeghal M, Adboun T, Kokkali P, Madabhushi G, Haigh S, Burali d' Arezzo F, Madabhushi S, Hung WY, Lee CJ, Chegn HC, Iai S, Tobita T, Zhou YG, Chen Y, Sun ZB, Manzari MT. Leap-GWU-2015 Experiment Specifications, Results, and Comparisons. Soil Dynamics and Earthquake Engineering, 2018, 113, p616-628.

Kutter, B. L. Effects of capillary number, Bond number, and gas solubility on water saturation of and specimens, Canadian Geotechnical Journal, Vol. 50 n°2, 2013,pp. 133-144.

Okamura M, Inoue T. 2012b. Preparation of fully saturated model for liquefaction study. Int. J. Phys. Model. Geotech 2012; 12(1):39–46.